Orientation of the Infrared Transition Moments for an α-Helix

Derek Marsh, Martin Müller, and Franz-Josef Schmitt
Max-Planck-Institut für biophysikalische Chemie, Abteilung Spektroskopie, D-37070 Göttingen, and Institut für Polymerforschung, D-01005 Dresden, Germany

ABSTRACT Appropriate values for the orientation of the amide transition dipoles are essential to the growing use of isotopically edited vibrational spectroscopy generally in structural biology and to infrared dichroism measurements on membrane-associated α-helices, in particular. The orientations of the transition moments for the amide vibrations of an α-helix have been determined from the ratio of intensities of the A- and E_1-symmetry modes in the infrared spectra of poly(γ-methyl-L-glutamate)$_x$-co-(γ-*n*-octadecyl-L-glutamate)$_y$ oriented on silicon substrates. Samples possessing a high degree of alignment were used to facilitate band fitting. Consistent results were obtained from both attenuated total reflection and transmission experiments with polarized radiation, yielding values of $\Theta_I = 38°$, $\Theta_{II} = 73°$, and $\Theta_A = 29°$, relative to the helix axis, for the amide I, amide II, and amide A bands, respectively. The measurements are discussed both in the context of the somewhat divergent older determinations, and in relation to the helix geometry and results on model amide compounds, to resolve current uncertainties in the literature.

INTRODUCTION

Determination of the orientation of the secondary structural elements of proteins and peptides in membranes from dichroism measurements on the amide infrared bands requires knowledge of the direction of the vibrational transition moments relative to the molecular axes (see, e.g., Tamm and Tatulian, 1997; Axelsen and Citra, 1996; Marsh, 1999). For helical polypeptides, the resultant transition moments are oriented either parallel or perpendicular to the helix axis (Miyazawa, 1960). However, when these parallel and perpendicular components practically coincide in frequency, or whenever integration is performed over the entire amide band, the ensuing vector summation of the parallel and perpendicular transition moments results in dichroic ratios that depend on the orientation, Θ, of the transition moment of an individual peptide group relative to the helix axis (Marsh, 1997). This is often the case for the amide I band of an α-helix, where the parallel and perpendicular components are separated in frequency by only $\sim 5\ cm^{-1}$, for the A- and E_1-modes, ($\nu_\parallel(0)$ and $\nu_\perp(\pm\chi)$, respectively). Also of increasing importance is the use of site-directed dichroism, in which isotope shifts decouple the local vibrational modes from those of the nonisotopically edited sections of the helix (Arkin et al., 1997). For the latter, however, consideration of nonaxiality, arising both from geometrical factors (Marsh, 1998) and from raising of the degeneracy of the E_1-modes, also becomes of importance. Uncertainty in the value of Θ for the amide I band of the α-helix therefore contributes materially to the accuracy in determining the orientation of α-helical proteins and peptides from the dichroism of the commonly used amide I band (see, e.g., Arkin et al., 1995; Citra and Axelsen, 1996). There is by no means universal accord in the values adopted for Θ by the various workers in the field, as pointed out, for instance, by Axelsen et al. (1995) and Bechinger et al. (1999).

Measurements of the direction of the amide I transition moments that are normally used for such orientational studies have all been carried out on unaxially oriented samples (the so-called "fibre orientation") and require corrections to the dichroic ratios that allow for the degree of misalignment or orientational distribution in the sample (Fraser and MacRae, 1973; Bradbury et al., 1962). The uncertainty in this correction contributes, at least in part, to the rather wide distribution of experimental values that appear in the literature. For the amide I band of the α-helix, values of $\Theta_I = 29–34°$ (Miyazawa and Blout, 1961), $\Theta_I = 39°$ (Tsuboi, 1962), and $\Theta_I = 40°$ (Bradbury et al., 1962) have been variously obtained, and are those routinely quoted in contemporary Fourier transform infrared (FTIR) dichroism studies. An alternative strategy is to estimate the transition moment orientations from dichroism measurements on single crystals of model amide compounds, combined with geometrical relations for the α-helix (Rothschild and Clark, 1979). This can result in a considerable range of uncertainty ($\Theta_I = 20–32°$ for the amide I), and values that differ substantially from those obtained from more direct experiments. A reason for the latter could be that the hydrogen bonding in the amide model compounds differs in detail from that in the secondary structure of peptides and proteins.

A way to measure the orientations of the transition moments that avoids uncertainties arising from the degree of alignment or orientation, is to use the integrated intensities of the parallel- and perpendicular-polarized resultant components for a given amide band (Miyazawa and Blout, 1961; Fraser and MacRae, 1973). For a regular helix, the resultant

Received for publication 1 September 1999 and in final form 25 January 2000.

Address reprint requests to Dr. Derek Marsh, Abt. 010 Spektroskopie, MPI für Biophysikalische Chemie, Am Fassberg 11, D-37077 Gottingen, Germany. Tel.: +49-551-201-1285; Fax: +49-551-201-1501; E-mail: dmarsh@gwdg.de.

0006-3495/00/05/2499/12 $2.00

transition moments of the parallel- and perpendicular-polarized components are determined by the projections of the transition moments of the individual peptide groups on the molecular symmetry axes of the polypeptide. The total integrated intensities of these components, therefore, may be used to obtain the orientation of the individual transition moments relative to the helix axis. This method was used previously by Suzuki (1967) with the parallel and perpendicular components of the amide I band of an antiparallel β-sheet fibrous protein. For the antiparallel β-sheet, the two components are well-separated in frequency, although the intensity of the parallel-polarized mode is rather low. Knowledge of the orientation of the individual transition moments, however, is not necessary for interpreting IR dichroism measurements in the β-sheet case (Marsh, 1997).

In the present work, we have used the above intensity method to determine the orientations of the peptide transition moments relative to the molecular symmetry axis of a regular α-helix. These results are significant not only for the determination of the orientation of α-helical proteins in membranes and in oriented protein systems in general, but also relate to the molecular structure of the α-helical polypeptide. A block copolymer, poly(γ-methyl-L-glutamate)$_x$-co-(γ-*n*-octadecyl-L-glutamate)$_y$, was chosen as a model polypeptide because previous experience has shown that members of this modified polyglutamate series are wholly α-helical and can be cast in films with a very high degree of orientation of the helical axis on polished silicon surfaces (Schmitt and Müller, 1997). The modified polyglutamate (PG_{30}) with mole fraction of long alkyl side chain, $y/(x + y) = 0.3$, was found to be near optimal for the latter purpose. Although, in principle, the degree of orientation is not a deciding factor for the method, a good orientation is particularly helpful in performing band fitting to determine the component intensities, especially for the amide I band. In addition, all side chain bands of these modified polyglutamates are well separated from the peptide backbone amide bands, which helps further in determining integrated intensities for the amide modes. These new determinations of the orientation of the transition moments then allow a critical re-evaluation of the rather diverse older measurements that currently are used for interpreting infrared dichroism measurements on oriented systems. Such considerations are of increasing importance with the recent introduction of site-directed, i.e., isotope-edited, IR dichroism in structural biology (Andersen et al., 1996; Arkin et al., 1997), although, in these systems, complications from lack of axial symmetry may require additional information on the orientation of the transition moments.

MATERIALS AND METHODS

Materials and sample preparation

Poly(γ-methyl-L-glutamate)$_x$-co-(γ-*n*-octadecyl-L-glutamate)$_y$ (PG_{30}, x:y = 7:3) was kindly supplied by G. Wegner, Mainz, Germany (Duda et al., 1988). Sample preparation was as described previously (Schmitt and Müller, 1997). Trapezoidal silicon internal reflection elements (IRE, 20 mm wide $\times$ 2 mm thick, upper and lower lengths 48 and 52 mm) with a 45° $\pm$ 1° aperture were used. Where appropriate, these were carefully polished in the direction of the short (20 mm) edge using a 0.2 μm diamond paste (Markon, Lotzwil, Switzerland). This resulted in visible parallel textures on the Si-surface. Scanning electron microscopy showed that the surface grooves created by polishing were smaller than 0.1 μm, as compared with mid-IR wavelengths of 10–2.5 μm. Thin films of PG_{30} were cast from a 0.1 wt % $CHCl_3$ solution onto the IRE surface and the solvent was left to evaporate. For achieving a highly oriented sample, the polyglutamate film was swollen under a $CHCl_3$ atmosphere, with subsequent evaporation of the solvent. The cast films exhibited interference colors (brown) that correspond to a film thickness in the region of 200 nm, which is less than the penetration depth of the incident IR radiation. (Calibration of the interference colors was established with Langmuir–Blodgett films of the peptide with defined thickness.)

FTIR measurements

The attenuated total reflection (ATR)-FTIR measurements were performed on an IFS 28 spectrometer (Bruker, Karlsruhe, Germany) with globar source and mercury cadmium telluride detector. A four-mirror ATR attachment (Perkin Elmer, Überlingen, Germany) was used with a thermostated flow-through cell (kindly provided by Prof. U. P. Fringeli, Zurich, Switzerland) surrounding the IRE plate. The infrared beam was polarized (gold grid polarizer on a KRS 5 substrate; Specac, Orpington, U.K.) either parallel (p) or perpendicular (s) with respect to the plane of incidence and guided through the IRE, resulting in 11 active reflections on the coated side of the IRE with a 45° angle of incidence. For transmission measurements, a custom-built sample holder was used to support a silicon plate similar to that used in the ATR experiments. The holder was oriented such that the IR beam was incident normal to the surface of the IRE plate. The IR beam was polarized parallel or perpendicular to the direction of polishing of the silicon plate. For both techniques, polarized single-channel intensity spectra were recorded of the bare plate (I_0, reference) and of the coated plate (I, sample) by collecting 500–1000 scans, respectively. The polarized absorbance spectra (A_p, A_s) were obtained by ratioing the polarized intensities I and I_0 according to $A = -\log(I/I_0)$.

The electric field components (E_x, E_y, E_z) in the ATR sample, normalized to the incident values, were calculated using the thin (thick) film approximation (Harrick, 1967). The refractive indices used for this calculation are $n_1 = 3.5$ (silicon), $n_2 = 1.49$ (sample), and $n_3 = 1.0$ (air.)

Fitting amide band components

Band fitting was performed over the spectral range 1790–1490 cm^{-1}, which covers the amide I, amide II, and ester carbonyl bands. Bruker software was used, which performs least squares fitting according to the Levenberg–Marquardt algorithm. Component bandshapes with a 1:1 sum of Gaussian and Lorentzian contributions were used. Adjustable lineshape parameters for each component were: position (ν_o), half-width at half-height (HWHH), and relative area (a_o). Generally, a linear baseline with free adjustable slope was used as an additional fitting parameter.

Band component positions were first determined from second derivative spectra obtained with parallel and perpendicular polarized radiation, and also from dichroic difference spectra between the two polarizations. Both the amide I and amide II bands contain A and E_1 components (see later). The values of ν_o and HWHH of the various components were then refined by an unconstrained fitting of the polarized spectra from the polished sample, i.e., that which displays the best degree of orientation. For determination of a unique ν_o and HWHH parameter set with maximum sensitivity (see Table 1), only the major component of the amide I (i.e., E_1 in p-polarization and A in s-polarization) and of the amide II band (i.e., A in

TABLE 1 Results of band fitting of the parallel (A) and perpendicular (E_1) components of the amide I and amide II bands of the substituted polyglutamate PG_{30} in oriented films with parallel (*p*) and perpendicular (*s*) polarized radiation

	Amide I		Amide II		Amide A
	E_1	A	E_1	A	E_1 + A
Position (cm^{-1})	1657.0	1651.8	1548.9	1517.0	3288
HWHH (cm^{-1})	15.2	14.2	20.0	20.0	60.5 (p) 58.5 (s)
A_p^{ATR}	1.40 ($\mp$0.12)*	0.29 ($\pm$0.13)*	2.26 ($\pm$0.01)*	0.16 ($\pm$0.12)*	1.31
A_s^{ATR}	0.66 ($\mp$0.54)*	4.59 ($\pm$0.44)*	0.33 ($\mp$0.02)*	0.19 ($\mp$0.02)*	5.35
A_p^T	0.28 ($\mp$0.04)*	0.16 ($\pm$0.03)*	0.35 ($\mp$0.0015)*	0.07 ($\pm$0.003)*	0.55
A_s^T	0.29 ($\mp$0.10)*	0.73 ($\pm$0.09)*	0.14 ($\mp$0.006)*	0.11 ($\mp$0.0015)*	1.28

Integrated intensities are given for ATR experiments (A_p^{ATR} and A_s^{ATR}) and for transmission experiments (A_p^T and A_s^T). Additional data are given for the total intensity (E_1 + A) of the amide A band.

*Ranges represent the results of suboptimal fits obtained by shifting the component frequencies given by ± 0.5 cm^{-1}. These ranges are much greater than the fitting error of the optimal fit (typically $\sim\pm 0.005$–± 0.01).

p-polarization and E_1 in *s*-polarization) was considered. For final quantification of the relative areas of the A and E_1 components in the p- and s-polarized spectra, the parameters ν_o and HWHH were kept constant at the values given in Table 1 and only the relative areas were allowed to relax.

The fitting errors were small, typically in the range of 0.2–2%, and maximally 4% for weak components. To obtain an estimate of the reliability of the fitted values, the band component positions were shifted by ± 0.5 cm^{-1} from the optimal values, and then fits were performed with these positions fixed. Differences in the total band intensity between the two fits were in one case comparable to, and in all other cases considerably greater than, the fitting error of the optimal fit. This procedure is therefore likely to establish an upper bound for the uncertainty in the optimal fits. Note that the deviations are correlated, because each fit must be performed with a consistent set of components.

THEORETICAL RESULTS

Parallel and perpendicular vibrational modes of an α-helix

Adopting the nomenclature of Zbinden (1964), which was used previously (Marsh, 1997, 1998), the mutually orthogonal molecular axes are designated *a*, *b*, and *c*, where *c* lies along the axis of the helix (see Fig. 1). The transition moment, **m**, of an individual peptide group makes an angle Θ with the helix *c*-axis and has an azimuthal orientation ϑ with respect to the orthogonal *a*-axis. The magnitudes of the resultant parallel and perpendicular transition moments of the helix are given, respectively, by

$$|M_\parallel|^2 \equiv M_c^2 \tag{1}$$

and

$$|M_\perp|^2 = M_a^2 + M_b^2 \tag{2}$$

where M_a, M_b, and M_c are proportional to the projections of **m** on the corresponding molecular axes. Thus $M_a \sim m \sin\Theta \sin\vartheta$, $M_b \sim m \sin\Theta \cos\vartheta$ and $M_c \sim m \cos\Theta$ (see Fig. 1), and the ratio of the total integrated intensities of the perpendicular and parallel polarized modes is simply

$$\frac{A_{tot}(\nu_\perp)}{A_{tot}(\nu_\parallel)} = \frac{k_\perp\langle|M_\perp|^2\rangle}{k_\parallel\langle|M_\parallel|^2\rangle} = \frac{k_\perp}{k_\parallel}\tan^2\Theta, \tag{3}$$

where $k_\perp$ and $k_\parallel$ allow for frequency-dependent differences in the absorption intensity of the $\nu_\perp$- and $\nu_\parallel$-modes. For an α-helix, $\nu_\perp$ is the E_1 mode and $\nu_\parallel$ is the A mode. The ratio $k_\perp/k_\parallel$ is reasonably close to unity and therefore is frequently ignored. With this latter assumption, Eq. 3 still differs, in a factor of two, from that usually presented for the ratio of the absorption intensities with radiation polarized perpendicular

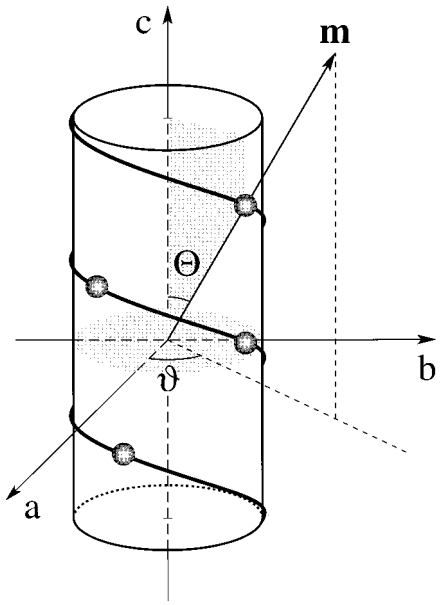

FIGURE 1 Orientation of an individual amide transition moment, **m**, relative to the molecular axis of an α-helix. The resultant amide transition moments of the entire helix, $\mathbf{M}_\parallel$ and $\mathbf{M}_\perp$ are oriented either parallel or perpendicular, respectively, to the *c*-axis.

and parallel to the molecular axis (Fraser, 1953; Fraser and MacRae, 1973). This is because it refers to the *total* intensity of the perpendicular polarized mode, rather than to that measured in a transmission experiment with normal incidence. The present formulation is completely general, i.e., independent of the experimental geometry, and therefore is more convenient when it comes to comparison with ATR measurements, as will be seen below.

The frequency-dependent factors, $k_\perp$ and $k_\parallel$, arise in Eq. 3 because the transition probability is proportional to the square of the frequency, and the populations of the vibrational modes are determined by the thermal Boltzmann factor. The normalization factor required is therefore given by: $k_\perp/k_\parallel = (\nu_\perp/\nu_\parallel)^2 \times \exp(h\nu_\parallel/kT)/\exp(h\nu_\perp/kT)$. For the A and E_1 modes of the amide I band, this amounts to only a 2% correction, because the two frequencies are close. For the amide II band, the $k_\perp/k_\parallel$ ratio corresponds to a 12% correction, but nonetheless has a relatively small effect ($\sim$1°) on the orientation, Θ, derived for the transition moment.

Determination of intensities of band components

ATR experiment

For a conventional ATR setup, the *z*-axis is defined as perpendicular to the orienting ATR plate, the *x*-axis lies in the propagation direction of the infrared beam and the *y*-axis is orthogonal to the plane of incidence (see Fig. 2, *lower*). The absorption intensity of a given band component, *i*, is proportional to $\langle(\mathbf{M}_i \cdot \mathbf{E})^2\rangle$, where $\mathbf{E} = (E_x, E_y, E_z)$ is the electric field vector of the infrared beam in the sample and $\mathbf{M}_i = (M_{x,i}, M_{y,i}, M_{z,i})$ is the transition moment of the absorbing vibrational mode. It is understood that the components of **E** are normalized to those of the incident beam. Angular brackets indicate summation over the orientational distribution in the sample. For radiation polarized in the plane of incidence (i.e., p-polarized), the integrated absorption is

$$A_{p,i}^{ATR} = k_i\langle(\mathbf{M}_{p,i} \cdot \mathbf{E}_p)^2\rangle = k_i(\langle M_{x,i}^2\rangle E_x^2 + \langle M_{z,i}^2\rangle E_z^2), \quad (4)$$

and, for radiation polarized perpendicular to the plane of incidence (i.e., s-polarized),

$$A_{s,i}^{ATR} = k_i(\mathbf{M}_{s,i} \cdot \mathbf{E}_s)^2 = k_i\langle M_{y,i}^2\rangle E_y^2, \quad (5)$$

where k_i is a constant for a given mode, *i*. In Eq. 4, it is assumed that the molecules are distributed randomly around the director axis (uniaxial orientation) and therefore the cross-terms drop out. Because the director lies along the *y*-axis, i.e., along the in-plane alignment direction, in the present experiments (see Fig. 2), uniaxial symmetry results further in the equality $\langle M_{x,i}^2\rangle = \langle M_{z,i}^2\rangle$. The magnitude of the total transition moment, $|M_i|$, of a given band component

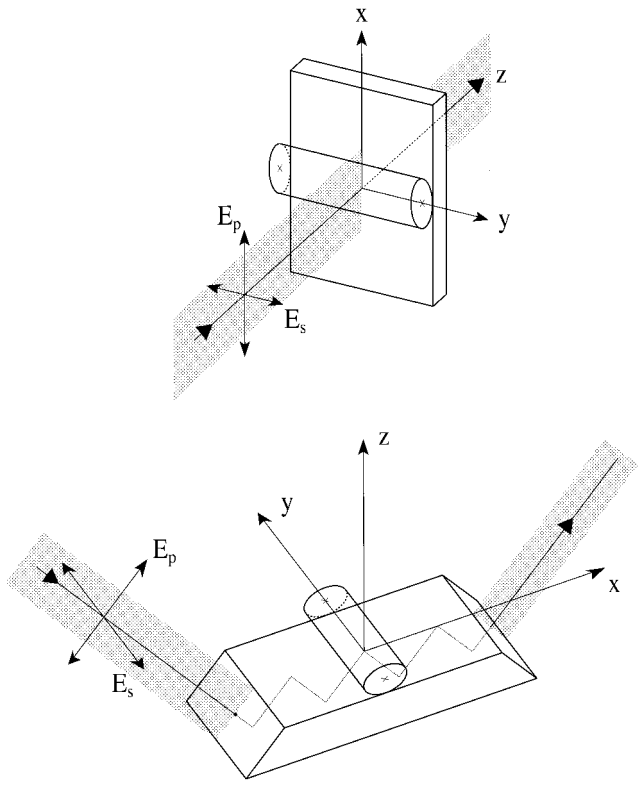

FIGURE 2 Geometric relations of the incident radiation to the orienting plane in an ATR experiment (*lower*) and in a transmission experiment (*upper*). The *z*-axis lies along the normal to the supporting plate, the *x*-axis is orthogonal to the *z*-axis and lies in the plane of incidence, and the *y*-axis is perpendicular to the plane of incidence. The radiation electric field vectors polarised parallel and perpendicular to the plane of incidence are E_p and E_s, respectively. In the present experiments, the polypeptide (indicated schematically by the cylinder) is preferentially oriented with the *y*-axis as director, which is the direction of polishing of the silicon plate in the ATR experiment.

with frequency ν_i is therefore given by the vector sum,

$$\langle M_i^2\rangle = \langle M_{x,i}^2\rangle + \langle M_{y,i}^2\rangle + \langle M_{z,i}^2\rangle$$
$$= k_i^{-1}[2A_{p,i}^{ATR}/(E_x^2 + E_z^2) + A_{s,i}^{ATR}/E_y^2], \quad (6)$$

which can be used to relate the total intensity of mode *i* to the ATR observables $A_{p,i}^{ATR}$ and $A_{s,i}^{ATR}$.

For an α-helical polypeptide, the ratio of the integrated total absorption intensities of the perpendicular, $\nu_\perp(\pm\chi)$, and parallel, $\nu_\parallel(0)$, polarized modes is given from Eq. 6, together with the first part of Eq. 3, by

$$\frac{A_{tot}[\nu_\perp(\pm\chi)]}{A_{tot}[\nu_\parallel(0)]} = \frac{2E_y^2A_p^{ATR}(\nu_\perp) + (E_x^2 + E_z^2)A_s^{ATR}(\nu_\perp)}{2E_y^2A_p^{ATR}(\nu_\parallel) + (E_x^2 + E_z^2)A_s^{ATR}(\nu_\parallel)}$$

(*y*-axis director), (7)

where $\nu_\parallel(0)$ is the A mode and $\nu_\perp(\pm\chi)$ is the E_1 mode of the α-helix. Eq. 7 applies to the *y*-axis as director, which is appropriate to the present experiments. For the sake of

completeness, the corresponding expression for the director aligned along the *z*-axis, which is the common situation with oriented membranes, is

$$\frac{A_{tot}[\nu_\perp(\pm\chi)]}{A_{tot}[\nu_\parallel(0)]} = \frac{E_y^2 A_p^{ATR}(\nu_\perp) + (2E_z^2 - E_x^2)A_s^{ATR}(\nu_\perp)}{E_y^2 A_p^{ATR}(\nu_\parallel) + (2E_z^2 - E_x^2)A_s^{ATR}(\nu_\parallel)}$$

(*z*-axis director). (8)

This latter equation should prove useful for similar ATR intensity measurements on oriented membranes.

Transmission experiment

For a simple transmission experiment with radiation at normal incidence to the oriented film, the *y*- and *x*-axes in the plane of the film will be perpendicular and parallel to the plane of incidence, respectively, assuming similar film-fixed axes (*x*, *y*, *z*) as in the ATR experiment (see Fig. 2, *upper*). The electric field vector components of the radiation in the film, normalized to those at incidence, are then $E_x = |\mathbf{E}_p|$, $E_y = |\mathbf{E}_s|$ and $E_z = 0$, where $|\mathbf{E}_p| = |\mathbf{E}_s|$. Correspondingly, the integrated absorptions for p-polarized and s-polarized radiation, respectively, are

$$A_{p,i}^T = k_i \langle M_{x,i}^2 \rangle E_x^2 \quad (9)$$

$$A_{s,i}^T = k_i \langle M_{y,i}^2 \rangle E_y^2 \quad (10)$$

in the transmission experiment. The director is again taken to lie along the *y*-axis, and axial symmetry about the *y*-axis therefore again results in $\langle M_{z,i}^2 \rangle = \langle M_{x,i}^2 \rangle$. Corresponding to Eq. 7, the ratio of the total integrated absorption intensities of the perpendicular, $\nu_\perp(\pm\chi)$, and parallel, $\nu_\parallel(0)$, polarized modes of an α-helix is then

$$\frac{A_{tot}[\nu_\perp(\pm\chi)]}{A_{tot}[\nu_\parallel(0)]} = \frac{2A_p^T(\nu_\perp) + A_s^T(\nu_\perp)}{2A_p^T(\nu_\parallel) + A_s^T(\nu_\parallel)} \quad (y\text{-axis director}) \quad (11)$$

for a transmission experiment. The transmission method, therefore, has the advantage that the values of the electric field vector components are not required explicitly, but, unfortunately, the signal-to-noise ratio is not as good as in the ATR experiment. (Transmission experiments with normal incidence are inappropriate for oriented membranes because of the axial symmetry about the *z*-axis.)

Molecular orientation

ATR experiment

For oriented membrane systems, molecular ordering occurs with the director aligned along the *z*-axis. The expression for the order parameter of the helix axis in this situation is well known (see e.g. Marsh, 1997). For the oriented polypeptide films studied here, however, the *y*-axis is the director (see Fig. 2). The components of the transition moment for this orientation of the director can be obtained from the expressions given by Marsh (1997) by making the transformation $(x, y, z) \rightarrow (z, x, y)$. With the usual assumption of axial symmetry about the helix axis (cf. Marsh, 1998), the dichroic ratio is given from Eqs. 4 and 5 by $R_y^{ATR} = (\langle M_x^2 \rangle / \langle M_y^2 \rangle)(E_x^2 + E_z^2)/E_y^2$. The order parameter for the director oriented along the *y*-axis, derived in the same way as that given previously for the director oriented along the *z*-axis (Marsh, 1997), is

$$\langle P_2(\cos\gamma) \rangle = \frac{E_x^2 + E_z^2 - E_y^2 R_y^{ATR}}{P_2(\cos\Theta)[E_x^2 + E_z^2 + 2E_y^2 \cdot R_y^{ATR}]}. \quad (12)$$

Where $P_2(x) = \frac{1}{2}(3x^2 - 1)$ is the second-order Legendre polynomial and R_y^{ATR} $(= A_p^{ATR}/A_s^{ATR})$ is the dichroic ratio determined by ATR. Here, γ is the angle that the helix axis makes with the *y*-axis. Eq. 12 is in agreement with the expression given by Fringeli et al. (1976) for this particular orientation of the director.

For A-type vibrational modes of the α-helix: $\Theta = 0°$, and from Eq. 12, the ATR dichroic ratio is given by

$$R_y^{ATR}(\Theta = 0°) = \frac{1}{2}\left[\frac{1}{\langle \cos^2\gamma \rangle} - 1\right]\left(\frac{E_x^2 + E_z^2}{E_y^2}\right). \quad (13)$$

Correspondingly, for an E_1-mode of the α-helix: $\Theta = 90°$, and the dichroic ratio is given by

$$R_y^{ATR}(\Theta = 90°) = \left[\frac{1}{1 - \langle \cos^2\gamma \rangle} - \frac{1}{2}\right]\left(\frac{E_x^2 + E_z^2}{E_y^2}\right). \quad (14)$$

When the A and E_1 modes of a given amide band can be resolved, these latter two equations may be used instead of Eq. 12 to determine the helix orientation. They have the advantage that they do not require knowledge of the angle Θ and, therefore, can be used to check the assumption of uniaxial symmetry (i.e., a single director) that was used in deriving them. It can readily be shown (cf. Marsh, 1997) that addition of the intensities of the A- and E_1-modes, with relative contributions, E_1/A, that are given by Eq. 3, yields a dichroic ratio, $R_y^{ATR}(E_1 + A)$, for the total integrated intensity of a given amide band that is identical with that obtained from Eq. 12, where Θ is the orientation of an individual peptide transition moment.

Transmission experiment

For normal incidence in a transmission experiment, and with the film axes as defined previously, the dichroic ratio is given from Eqs. 9 and 10 simply by $R_y^T = \langle M_x^2 \rangle / \langle M_y^2 \rangle$. Corresponding to Eq. 12 the order parameter in terms of the transmission data is given by:

$$\langle P_2(\cos\gamma) \rangle = \frac{1 - R_y^T}{P_2(\cos\Theta)[1 + 2R_y^T]}, \quad (15)$$

where $R_y^T = A_p^T/A_s^T$. For the A-type and E_1-type modes of an α-helix, the dichroic ratios in the transmission experiment are then given by expressions identical to those of Eqs. 13 and 14, respectively, where $(E_x^2 + E_z^2)/E_y^2$ is equal to one.

EXPERIMENTAL RESULTS

Transition moment orientation from intensities

ATR experiment

Band fitting to the amide regions of the ATR-FTIR spectra of PG_{30} with radiation polarized parallel and perpendicular to the plane of incidence are given in Fig. 3 *A*. The high degree of orientation of the sample is seen from the large dichroism of the amide bands in these spectra. It is evident that the contribution to the polarized spectra of the component with complementary polarization is small. The consequence of this is a clear shift in frequency of the amide I maximum between the different polarizations, and good resolution of the two modes in the amide II region. Band fitting to the A- and E_1 components, as described in Materials and Methods, is therefore possible even for the amide I band. This is illustrated in Fig. 3 *A*. Overall, the rather narrow bandwidths, the symmetry of the component bands, and the high degree of ordering achieved, suggest that the α-helices are highly regular.

The numerical results of the band fitting are given in Table 1. The ratio of total intensities of the perpendicular and parallel components calculated from Eq. 7 by using the data of Table 1 is $A_{tot}(E_1)/A_{tot}(A) = 0.613$ and 9.16 for the amide I and amide II bands, respectively. By using Eq. 3, this gives values of $\Theta_I = 38.3°$ ($\pm 5.3°$) and $\Theta_{II} = 72.7°$ ($\pm 0.4°$) for the orientations of the amide I and amide II transition moments, respectively, relative to the helix axis. The ranges in parentheses represent the result of deviations in the fits obtained by shifting the component center frequencies by ± 0.5 cm^{-1} from the optimal value (see Materials and Methods, and Table 1). As already stated, these are really upper bounds for the uncertainty in fitting and are much greater than the fitting errors. The above values of Θ_I and Θ_{II} were calculated using the thin-film approximation for the electric field intensities (Harrick, 1967). Using the thick-film approximation yields corresponding values of 33° and 71° for the amide I and amide II bands, respectively. As seen below and from the data given in Materials and Methods, the thin-film approximation is more appropriate. It should be noted that the method of evaluation based on Eqs. 3 and 7 is rather stable for highly ordered ATR samples, such as those used here (see later). Even if the samples were perfectly ordered, i.e., $A_s(E_1) = 0 = A_p(A)$, the values of Θ_I and Θ_{II} would be changed by only

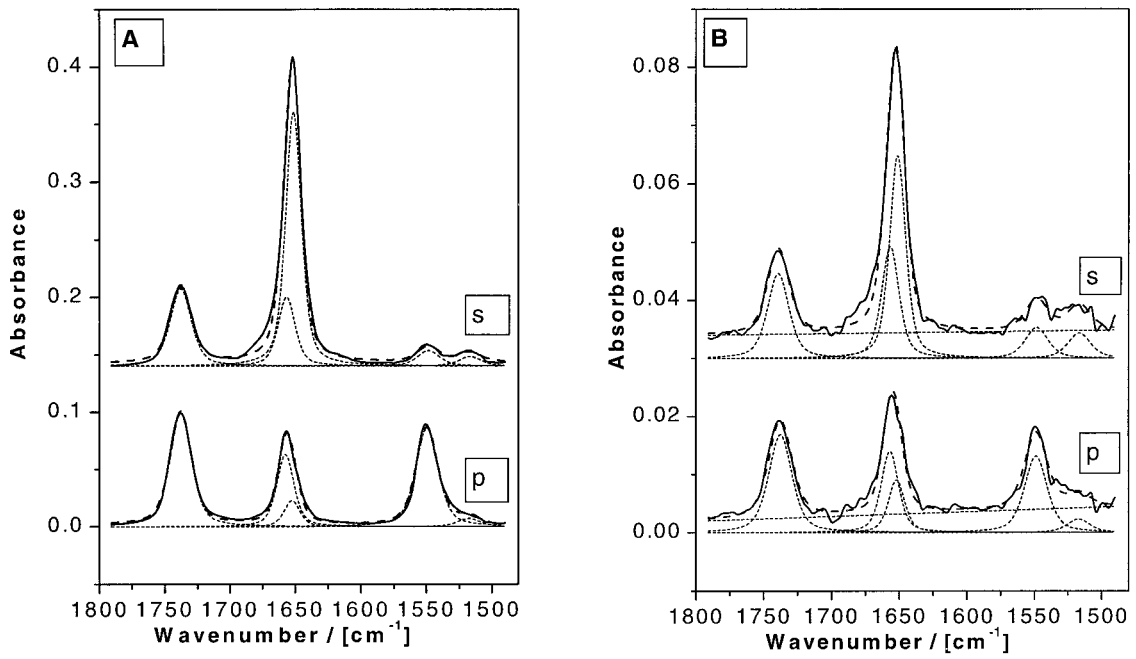

FIGURE 3 Band fitting in the amide I, amide II, and carbonyl regions of the mid-IR spectrum from a film of the modified polyglutamate PG_{30} that was oriented: (*A*) on a silicon ATR plate that was polished in the *y*-direction (perpendicular to the plane of incidence), and (*B*) on the window of a silicon transmission cell oriented normal to the plane of incidence. ATR spectra (*A*) and transmission spectra (*B*) are shown for *upper:* radiation polarized perpendicular to the plane of incidence (s-polarization) and *lower:* radiation polarized parallel to the plane of incidence (p-polarization). Solid lines represent the original spectra, long dashes are the spectral fit, and short dashes are the individual fitted components. For transmission spectra, the fitted baseline is also shown.

1° in the thin-film approximation, when the total band area is maintained constant.

The above results were confirmed by ATR measurements on an independent sample that was less well ordered. The lower degree of ordering resulted from using a silicon IRE wafer that was not specifically polished. Spontaneous orientation of the polymer axes was mediated, in this case, only by intrinsic texture of the surface that was not detected visually. Band fitting, as described above, yielded orientations of the transition moments that were consistent with those derived from the more highly ordered sample. For three samples, including two with lower degrees of order, the mean values obtained were: $\Theta_I = 35 \pm 3°$ and $\Theta_{II} = 72 \pm 2°$. Most weight should be placed on the highly oriented sample, however, because, for this, the method is most stable, as noted above.

Transmission experiment

Band fitting to the amide regions of the transmission FTIR spectra of PG_{30} with radiation polarized parallel and perpendicular to the plane of incidence are given in Fig. 3 *B*. The marked dichroism is qualitatively similar to that in the ATR experiment (given in the same figure) because the director of the oriented film has the same orientation (i.e., perpendicular) to the plane of incidence. The signal-to-noise ratio is not as good as achieved in the ATR experiment. However, it is important to analyze these data to resolve potential uncertainties regarding the estimates of the electric field intensities in the ATR experiment. The integrated intensities obtained from the band fitting of the polarized transmission spectra, by using the fitting parameters established from the ATR experiment, are presented in Table 1. The ratio of the total intensities of the E_1 and A modes calculated from Eq. 11 results in orientations $\Theta_I = 42 \pm 5°$ and $\Theta_{II} = 63 \pm 0.5°$ for the transition moments of the amide I and amide II modes, respectively, from the transmission experiment. Again, Eq. 3 is used to determine the orientation. The value for the amide I mode is in agreement with that obtained from ATR by using the thin-film approximation, hence justifying the use of the latter in this case. Less good agreement is obtained for the amide II transition moment, which can be traced to the poor signal-to-noise ratio in this region of the transmission spectrum (see Fig. 3 *B*). For instance, if it is assumed that $A_p^T(A) = 0$ as opposed to the fitted value of $A_p^T = 0.066$ given in Table 1 (which is almost justified by the data—see Fig. 3 *B*), a value of $\Theta_{II} = 71°$ is obtained from the transmission experiment, close to that obtained by ATR.

Molecular orientation

Calculation of the integrated intensities of the E_1 and A modes from the ATR measurements was made by assuming uniaxial symmetry about the director axis, in deriving Eq. 7. Comparison of the molecular orientations obtained from the dichroic ratios of the amide I and amide II bands provides a useful check on this assumption.

For the amide I band, the A mode ($\nu_{\|}(0)$) is far the stronger, and for this mode, $\Theta = 0°$. Using the ATR data from Table 1 for this mode, together with Eq. 13, yields a value of $\langle\cos^2\gamma\rangle = 0.90$ (∓ 0.03), giving an order parameter of $\langle P_2(\cos\gamma)\rangle = 0.85$ (∓ 0.05) for the helix axis. Correspondingly, for the amide II band, the E_1 mode ($\nu_{\perp}(\pm\chi)$) is the stronger, and for this mode, $\Theta = 90°$. Using the dichroic ratio for the E_1 mode of the amide II band, together with Eq. 14, yields a value of $\langle\cos^2\gamma\rangle = 0.85$ (± 0.01), i.e., an order parameter for the helix of $\langle P_2(\cos\gamma)\rangle = 0.77$ (± 0.02).

In each case, the thin-film approximation is used for determining the strength of the electric field vector components. These values of $\langle\cos^2\gamma\rangle$ illustrate the high degree of uniaxial order in these samples, and their relative consistency suggests that the axial approximation is reasonable for this system. Using the thick-film approximation produces considerably more divergent values, and therefore the thin-film approximation is again favored.

Less good order was achieved in the samples used for transmission experiments, at least in part because the IRE was not polished in this case. However, applying the same procedure with Eq. 15 and the transmission data from Table 1 again yields consistent values of $\langle\cos^2\gamma\rangle = 0.69$ and 0.68 for the A mode of the amide I and the E_1 mode of the amide II band, respectively, further supporting the axial approximation.

Transition moment orientation from dichroic ratios

For the amide A band, the positions of the bands with parallel and perpendicular polarized radiation are within 2 cm^{-1} of each other, and the bands are broad, so that band fitting to the A and E_1 modes separately is not possible. The total integrated intensities of this band (i.e., $A + E_1$) are given in Table 1 for both ATR and transmission experiments. The resulting dichroic ratios may be used to obtain an estimate of the transition moment orientation from Eq. 12 for ATR, together with the corresponding value of the helix order parameter $\langle P_2(\cos\gamma)\rangle = 0.85$ that is obtained from the dichroic ratio of the A mode of the amide I band. The latter is most appropriate because this band has the greater sensitivity to Θ. The resulting orientation of the amide A transition moment is $\Theta_A = 29.2°$ ($\mp 1.7°$) obtained from the ATR measurements. The range in parentheses corresponds to the change in amide I dichroic ratio obtained from suboptimal fits that are produced by shifting the amide I component positions by ± 0.5 cm^{-1}. An error of ± 0.05 in helix order parameter changes the value of Θ_A by $\mp 2°$. Applying the same procedure to the total intensities of the amide I and amide II bands, by using the data given in Table 1, results

in values of $\Theta_I = 34°$ ($\mp 0.9°$) and $\Theta_{II} = 74°$ ($\pm 3.0°$), respectively. These latter values are in reasonable agreement with those obtained from the ATR intensities. Again the ranges in parentheses result from a ± 0.5 cm^{-1} shift from the optimum positions of the amide I or amide II band components, respectively. A small correction for the frequency dependence was also made, as already described, in the summation of the band component intensities.

The helix order parameter obtained from the A mode of the amide I band in the transmission experiments is $\langle P_2(\cos\gamma)\rangle = 0.49$. Using this order parameter, together with Eq. 15 and the dichroic ratio of the amide A band in transmission, yields a value of $\Theta_A = 29.7°$. This is in good agreement with the orientation of the amide A transition moment obtained by the same method from the ATR measurements, even though the degree of order of the two samples differs.

DISCUSSION

The subject of this paper has considerable relevance in modern structural biology. The application of polarized ATR-FTIR to the determination of protein orientation is steadily increasing, and will increase further with the recent introduction of isotopic editing. However, the interpretation of such experiments still relies on basic measurements of the orientation of the amide transition moments that were made before the advent of Fourier transform instrumentation, and among which there is significant disagreement.

Most previous work has made use of dichroic ratios (Bradbury et al., 1962; Miyazawa and Blout, 1961; Tsuboi, 1962). It is clear from Eq. 12 that assumptions about the degree of molecular orientation, $\langle P_2(\cos\gamma)\rangle$, are essential, if the orientation of the transition moment, $P_2(\cos\Theta)$, is to be determined by this method; also for transmission experiments. It will be seen immediately below that this has contributed materially to the apparent disagreement among the values quoted in the literature. Even if the dichroic ratios of two bands, e.g., the amide I and amide II, are combined, only the ratio of transition moment orientations, i.e., $P_2(\cos\Theta_I)/P_2(\cos\Theta_{II})$, can be determined. Use of the relative intensities of the A- and E_1-symmetry modes, as is done here, therefore, provides a valuable independent means of measurement which, as noted already, is rather stable for the amide I and amide II bands.

Comparison with previous measurements

The new measurements of the amide transition moment orientations that are reported here are compared with the various older determinations in Table 2. In the older measurements, dichroic ratios were determined from band heights, and intensities from heights and band widths. Here we have used band fitting and integration, with suitable baseline corrections.

TABLE 2 Orientations, Θ_M, of the individual transition moments of the amide bands of an α-helix, relative to the helix axis

Polypeptide*	Amide A	Amide I	Amide II	Reference
PG_{30}	29°	38°	73°	This work
PBG	27°, 29°	39°	74°, 76°	Tsuboi (1962)
PBA	18°	40°	—	Bradbury et al. (1962)
PBG	—	29°–34°	75–77°	Miyazawa and Blout (1961)

*PG_{30}, poly(methyl-L-glutamate)$_x$-co-(γ-*n*-octadecyl-L-glutamate)$_y$, *x*:*y* = 7:3, PBG, poly-γ-benzyl-L-glutamate; PBA, poly-β-benzyl-L-aspartate.

As already mentioned, most previous measurements of the amide I orientation have required a correction for the degree of orientation of the sample. In the measurements of Bradbury et al. (1962) and Tsuboi (1962) there was a degree of arbitrariness in the estimate of this correction. For instance, it was *assumed* by Bradbury et al. (1962) that the orientation of the amide A transition moment was $\Theta_A = 18°$, to calculate the degree of orientation for their poly-β-benzyl-L-aspartate (PBA) samples. If it is alternatively assumed that the PBA samples of Bradbury et al. (1962) were perfectly oriented, values of $\Theta_A = 25°$ and $\Theta_I = 42°$ are obtained for the amide A and amide I transition moments, respectively. Although absolutely perfect orientation is unlikely, these latter estimates are in better overall agreement with the trends in Table 2.

To make the orientation correction for measurements on poly-γ-benzyl-L-glutamate (PBG), Tsuboi (1962) took the dichroic ratio observed for the E_1-species component of the Amide II band, as an upper limit. The double entries in Table 2 correspond to evaluations from two samples with different degrees of orientation. The first of the two values for the amide A and amide II bands, and that for the amide I band, are derived from the more highly ordered sample. Assuming this sample to be perfectly ordered changes these values by less than 1° (Tsuboi, 1962). The agreement of these results with the present ones is mostly very satisfactory.

The determination of Θ_I by Miyazawa and Blout (1961) deviates most of the various values given for the amide I transition moment in Table 2. This range of values was determined from the amide I dichroic ratio, together with the helix orientation obtained from the dichroism of the E_1 mode of the amide II band, a procedure analogous to that used here for the amide A band. However, as pointed out by Bradbury et al. (1962), Miyazawa and Blout assumed a model of completely planar orientation for making the correction, rather than the uniaxial model used here and by others. If a uniaxial correction is used, based on Eq. 4, then the data of Miyazawa and Blout (1961) yield values of $\Theta_I = 33$–$37.5°$ that agree better with the other values in Table 2.

For the oversimplified case of the transition moments confined solely to the *x–y* plane, Eq. 7 then becomes

$$\frac{A_{tot}(\nu_\perp)}{A_{tot}(\nu_\parallel)} = \frac{E_y^2 A_p^{ATR}(\nu_\perp) + E_x^2 A_s^{ATR}(\nu_\perp)}{E_y^2 A_p^{ATR}(\nu_\parallel) + E_x^2 A_s^{ATR}(\nu_\parallel)}$$

(planar distribution). (16)

This planar distribution used by Miyazawa and Blout (1961) is realistic neither for α-helices nor for β-sheets, in that it can apply rigorously only to the $\nu_\parallel$ component. For a β-sheet, it could be a reasonable first approximation because the component of the transition moment perpendicular to the sheet is expected to be small (Miyazawa and Blout, 1961). This is not the case, however, for an α-helix, because the transition moments are distributed azimuthally around the helix axis. Nevertheless, it may be used to make an overestimate of the effect that an extreme nonaxiality in helix distribution may have. Applying Eqs. 3 and 16 to the present data from Table 1 yields values of $\Theta_I = 34°$ and $\Theta_{II} = 70°$ for ATR, using the thin-film approximation, and correspondingly $\Theta_I = 36°$ for transmission. It therefore can be concluded that a limited degree of nonaxiality will not affect our results presented in Table 2.

More recent data have been published by Citra and Axelsen (1996) and Bechinger et al. (1999) that are relevant to the orientation of the amide transition moments for an α-helix. Again, these measurements depend on the degree of order of the samples, and on other experimental conditions. Values of Θ_I consistently larger than 40° were suggested for PBA by the former authors, whereas a value closer to 30° was proposed for PBG. The latter authors obtained an upper bound for Θ_I of 39 ± 2° and a lower bound for Θ_{II} of 69°. With the exception of the rather low value for PBG, these results are consistent with the present measurements. Somewhat in contrast are theoretical calculations of dichroic ratios for the amide I and the amide II bands of an α-helix that were performed with the side chains represented as point masses (Reisdorf and Krimm, 1995). For a fiber orientation in transmission, the dichroic ratio is given by $R = 2\cot^2\Theta$ (Fraser, 1953; and see the discussion surrounding Eq. 3). This yields values of Θ_I = 29–30° and $\Theta_{II} = 76°$ for protonated amides, and $\Theta_I = 33°$ for deuterated amides, obtained from the theoretical dichroic ratios. Although of a similar magnitude, the theoretical predictions differ from the present results and most of those of Table 2 in the case of the amide I band.

Comparison with model compounds

The amide A, amide I, and amide II transition moments all lie in the peptide plane. Their orientations, δ_M, relative to the peptide carbonyl bond can be estimated by combining the FTIR measurements with information on the orientation of the peptide planes in an α-helix (see Fig. 4). It is necessary to know the inclination, α, of the peptide plane relative to the helix axis and the angle, β, between the carbonyl bond and the projection of the helix axis on the peptide plane. The orientation, Θ_M, of transition moment *M* relative to the helix axis is then given by

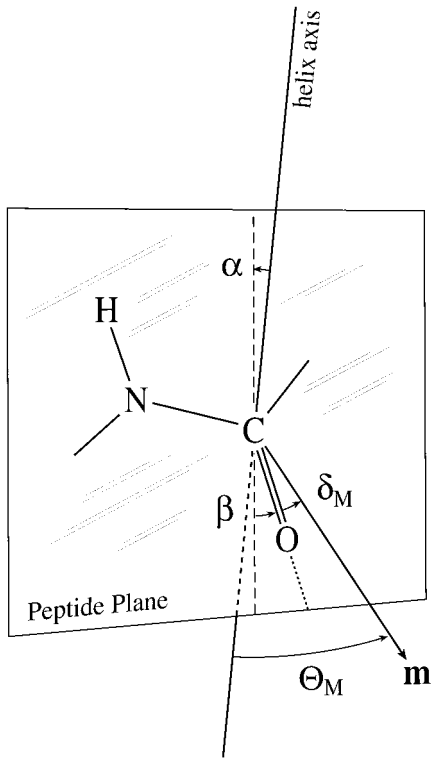

FIGURE 4 Orientations of the carbonyl bond (C═O) and an individual amide transition moment (**m**) in the peptide plane, and of the peptide plane relative to the axis of the α-helix. The carbonyl bond makes an angle β with respect to the projection of the helix axis on the peptide plane; the transition moment makes an angle δ_M with the carbonyl bond; and the peptide plane is tilted at an angle α to the helix axis.

$$\cos\Theta_M = \cos\alpha \cdot \cos(\beta + \delta_M), \quad (17)$$

where $\alpha = 6.1°$ and $\beta = 12.9°$ for α-poly-L-alanine, and $\alpha = 3.3°$ and $\beta = 14.5°$ for a standard right-handed α-helix (see Appendix). The values given in the Appendix are based on refined coordinates, whereas previous comparisons and estimates have relied on unrefined coordinates or used approximate ranges for α and β (Tsuboi, 1962; Rothschild and Clark, 1979). From the FTIR measurements given here and the data in the Appendix, the transition moments of the amide A, amide I, and amide II bands have orientations corresponding to $\delta_A = 16°$ (14.5°), $\delta_I = 25°$ (23.7°), and $\delta_{II} = 60°$ (58°), respectively, where the values in parentheses are those calculated using the parameters for an α-helix with standard stereochemistry. These values can be compared with those determined from single crystals of amide model compounds that are given in Table 3. There is rea-

TABLE 3 Orientations, δ_M, of amide band transition moments relative to the carbonyl bond, in the direction away from the CO—NH bond, for an α-helix and amide model compounds

Compound	Amide A	Amide I	Amide II	Reference
PG_{30}	+16°/14.5°*	+25°/23.7°* (1652, 1657)†	+60°/58°*	This work
N,N′-Diacetyl hexamethylene diamine	+8°	+17° (1632, 1642)†	+68°, +77°	Sandeman (1955)
Acetanilide	+13 ± 1.5°‡	+22 ± 2° (1666)†	+72°‡	Abbott and Elliot (1956)
N-Methyl acetamide	+8° or +28°	+15 to +25° (1645)†	+73°‡	Bradbury and Elliot (1963)

*Alternative values assuming α-poly-L-alanine/standard α-helix coordinates.
†Frequency of amide I band(s) in cm^{-1}.
‡Alternative orientation is discarded by comparison with *N,N′*-diacetylhexamethylenediamine, where no ambiguity exists.

sonable correspondence with the model compounds for the amide A and amide I bands, but not for the amide II band. The latter is a feature in common with all determinations of the transition moment for α-helical peptides, not just the present measurements. It should be noted that the hydrogen-bonding pattern in the amide model compounds can differ considerably from that in an α-helix and this may, at least in part, account for the large discrepancies in the case of the amide II band.

Inspection of the amide I frequencies of the model compounds that are given in Table 3 suggests that the above proposal is, in fact, the case. Acetanilide with a higher amide I frequency, more similar to that of α-helices, has a larger value of δ_I than that of *N,N′*-diacetylhexamethylenediamine, which has a lower amide I frequency that is close to that typical of β-sheet structures. In agreement with this trend, a value of $\delta_I = 19°$ has been determined for the antiparallel β-sheet structure of silk fibroin (Suzuki, 1967). Reference to Table 3 therefore suggests that the values of δ_I for the amide I of an α-helix are greater than those for a β-sheet structure because of the difference in H-bond strengths (and orientation) that is reflected in the characteristic amide frequencies. This further implies that the values of $\delta_I \sim 20°$ that have been adopted previously for estimating amide I band orientations for an α-helix (Fraser and MacRae, 1973; Rothschild and Clark, 1979) are probably too low. In choosing an appropriate model compound, attention should be paid to correlation with the amide frequencies, rather than assuming a mean value from the different model substances. For a β-sheet, *N,N′*-diacetylhexamethylenediamine provides a reasonable correspondence. For an α-helix, acetanilide (and possibly methyl acetamide) provides a more appropriate comparison. The present results for the amide I orientation, δ_I, are in reasonable agreement with the upper limits for these latter two model compounds. There is, however, a clear discrepancy between the orientation of the amide II transition moment of an α-helix and those of the model compounds that are given in Table 3. Presumably, the amide hydrogen bonding for none of the model corresponds exactly with that for an α-helix.

CONCLUSION

The present measurements were aimed to resolve some of the uncertainties currently surrounding the appropriate choice for the orientation of the transition moments of the amide bands that is needed in interpreting infrared dichroism measurements on α-helices. Motivations for this were both the growing application of site-directed FTIR spectroscopy in structural biology, and the necessity to re-evaluate critically the rather diverse older determinations that are presently adopted with little general consensus in the literature. One of the strategies used was to use the relative intensities of the A- and E_1-symmetry modes. This type of determination does not require knowledge of the degree of orientational ordering of the sample, and therefore is an independent measurement that can be compared with the more common procedure based on dichroic ratios. A further approach was to make selective comparison with results from amide model compounds, and to explore the uncertainty arising from using different refined coordinates for the α-helix. Different model compounds are appropriate to the α-helix and β-sheet structures. Taking into account the discrepant assumptions made in the various previous determinations, a reasonable degree of consistency that includes the present results can now be achieved.

Finally, it is appropriate to enquire to what extent measurements on dry α-helical peptides, including the present ones, are applicable to proteins in general. The values obtained for transition moment orientations refer to intrahelically H-bonded peptides in rather regular α-helices. Therefore, they should be reasonably representative of such structures in other environments. Differences might be expected, however, in situations where there are appreciable deviations from standard α-helical geometry and consequent changes in H-bonding strengths. In such situations, nonaxiality and nondegeneracy of the E_1 modes also may cause additional complications. Bacteriorhodopsin (Rothschild and Clark, 1979) is a possible case in point. The amide I band has an atypically high frequency (1667 cm^{-1}) for α-helices and the dichroic ratios are such that the amide I transition moment would be $\Theta_I = 36°$ if all helices were perfectly ordered. The recent high-resolution structure of

bacteriorhodopsin (Luecke et al., 1999) reveals that not all helices are perfectly aligned with the membrane normal. However, transmembrane helices B, C, and F contain proline-induced kinks, and helix G contains a π-bulge, all of which disrupt the regular α-helical hydrogen bonding. It should be noted, however, that other dichroic measurements on bacteriorhodopsin (Nabedryk and Breton, 1981; Draheim et al., 1991) do not necessarily imply such large departures in orientation of the amide I transition moment.

In the discussion of the results on model compounds, it was pointed out that the intrinsic orientations of the amide transition moments correlate with the band frequencies, i.e., with the H-bond strengths. The amide frequencies therefore give some indication as to whether the present results are applicable, and Table 3 provides a guide as to how large the deviations might be. In addition, the orientations, δ_M, that are given in Table 3 for a peptide-fixed coordinate system should help in making corrections for the purely geometrical effects of helix distortions. This will be particularly the case when single residues are resolved by isotopic editing, or, alternatively, when step-wise summation is made on a residue-by-residue basis (cf. Marsh, 1998).

APPENDIX: ORIENTATION OF THE PEPTIDE PLANE AND CARBONYL BOND IN AN α-HELIX

Cylindrical polar coordinates of the peptide unit in α-poly-L-alanine that are deduced from the refined coordinates of Arnott and Dover (1967) are given in Table A1. Corresponding coordinates for a right-handed α-helix with standard stereochemistry as refined by Parry and Suzuki (1969) are given in parentheses. The angle, $\Theta_{1,2}$, that the bond joining atoms 1 and 2 makes with the helix axis is given by

$$\tan\Theta_{1,2} = \frac{\sqrt{R_1^2 + R_2^2 - 2R_1R_2\cos(\phi_2 - \phi_1)}}{Z_1 - Z_2}. \quad \text{(A1)}$$

If α is the angle that the peptide plane makes with the helix axis, and $\beta_{1,2}$ is the angle that the 1—2 bond makes with projection of the helix axis on the peptide plane as defined in Fig. 4, then (cf. Eq. 17),

$$\cos\Theta_{1,2} = \cos\alpha \cdot \cos\beta_{1,2}. \quad \text{(A2)}$$

If $\tau_{1,2,3}$ is the angle between the 1—2 and 2—3 bonds, then the angle $\Theta_{2,3}$ that the 2—3 bond makes with the helix axis is similarly given by

$$\cos\Theta_{2,3} = \cos\alpha \cdot \cos(\beta_{1,2} + \tau_{1,2,3}), \quad \text{(A3)}$$

TABLE A1 Cylindrical polar coordinates for a peptide group in α-poly-L-alanine (Arnott and Dover, 1967)*

Atom	Z (nm)	R (nm)	φ (°)
C^α	0	0.2288 (0.2280)†	0
C′	0.1054 (0.1089)†	0.1664 (0.1645)†	27.16 (25.88)†
O	0.2256 (0.2288)†	0.1906 (0.1858)†	21.24 (18.15)†
N	0.0589 (0.0627)†	0.1548 (0.1550)†	72.22 (71.31)†

*h = 0.1495 nm, t = 99.57°, ω = −179.8°, $\tau(C^\alpha, C', O)$ = 121.0°, $\tau(O, C', N)$ = 123.6°.

†Standard right-handed α-helix as refined by Parry and Suzuki (1969), h = 0.15 nm, t = 100°, ω = 180°, $\tau(C^\alpha, C', O)$ = 121°, $\tau(O, C', N)$ = 125°.

TABLE A2 Orientations of the peptide plane (α) and carbonyl bond ($\Theta_{C',O}$) relative to the helix axis, and of the carbonyl bond ($\beta_{C',O}$) within the peptide plane, in α-poly-L-alanine and in a standard right-handed α-helix*

	α (°)	$\beta_{C',O}$ (°)	$\Theta_{C',O}$ (°)
α-poly-L-ala	6.1	12.9	14.2
α-helix	3.3	14.5	14.8

*Angles are defined in Fig. 4.

where the sign convention assumes that both bonds are inclined on the same side of the projection of the helix axis. Applying Eqs. A1–A3 to the data for the C′—O and C′—C^α bonds that are given in Table A1 results in the angular orientations given in Table A2. Consistent values of α and $\beta_{C',O}$ are also obtained from the data for the C′—O and C′—N bonds, because the peptide unit in the α-poly-L-alanine structure is very close to planar (Arnott and Dover, 1967).

REFERENCES

Abbott, N. B., and A. Elliot. 1956. Infra-red spectrum and dichroism of crystalline acetanilide. *Proc. Roy. Soc. A.* 234:247–268.

Anderson, T. S., J. Hellgeth, and P. T. Lansbury. 1996. Isotope-edited infrared linear dichroism—determination of amide orientational relationships. *J. Am. Chem. Soc.* 118:6540–6546.

Arkin, I. T., M. Rothman, C. F. C. Ludlam, S. Aimoto, D. M. Engelman, K. J. Rothschild, and S. O. Smith. 1995. Structural model of the phospholamban ion channel complex in phospholipid membranes. *J. Mol. Biol.* 248:824–834.

Arkin, I. T., K. R. MacKenzie, and A. T. Brünger. 1997. Site-directed dichroism as a method for obtaining rotational and orientational constraints for oriented polymers. *J. Am. Chem. Soc.* 119:8973–8980.

Arnott, S., and S. D. Dover. 1967. Refinement of bond angles of an α-helix. *J. Mol. Biol.* 30:209–212.

Axelsen, P. H., and M. J. Citra. 1996. Orientational order determination by internal reflection infrared spectroscopy. *Prog. Biophys. Mol. Biol.* 66: 227–253.

Axelsen, P. H., B. K. Kaufman, R. N. McElhaney, and R. N. A. H. Lewis. 1995. The infrared dichroism of transmembrane helical polypeptides. *Biophys. J.* 69:2770–2781.

Bechinger, B., J. M. Ruysschaert, and E. Goormaghtigh. 1999. Membrane helix orientation from linear dichroism of infrared attenuated total reflection spectra. *Biophys. J.* 76:552–563.

Bradbury, E. M., L. Brown, A. R. Downie, A. Elliot, R. D. B. Fraser, and W. E. Hanby. 1962. The structure of the ω-form of poly-β-benzyl-L-aspartate. *J. Mol. Biol.* 5:230–247.

Bradbury, E. M., and A. Elliott. 1963. The infra-red spectrum of crystalline *N*-methylacetamide. *Spectrochim. Acta*. 19:995–1012.

Citra, M. J., and P. H. Axelsen. 1996. Determination of molecular order in supported lipid membranes by internal reflection Fourier transform infrared spectroscopy. *Biophys. J.* 71:1796–1805.

Draheim, J. E., N. J. Gibson, and J. Y. Cassim. 1991. Dramatic in situ conformational dynamics of the transmembrane protein bacteriorhodopsin. *Biophys. J.* 60:89–100.

Duda, G., A. J. Schouten, T. Arndt, G. Lieser, G. F. Schmidt, C. Bubeck, and G. Wegner. 1988. Preparation and characterization of monolayers and multilayers of preformed polymers. *Thin Solid Films.* 159:221–230.

Fraser, R. D. B. 1953. The interpretation of infrared dichroism in fibrous protein structures. *J. Chem. Phys.* 21:1511–1515.

Fraser, R. D. B., and T. P. MacRae. 1973. Conformation in Fibrous Proteins and Related Synthetic Peptides. Academic Press, New York.

Fringeli, U. P., M. Schadt, P. Rihak, and H. H. Günthard. 1976. Hydrocarbon chain ordering in liquid crystals investigated by means of infra-

red attenuated total reflection (IR-ATR) spectroscopy. *Z. Naturforsch.* 31a:1098–1107.

Harrick, N. J. 1967. Internal Reflection Spectroscopy. Wiley, New York.

Luecke, H., B. Schobert, H.-T. Richter, J.-P. Cartailler, and J. K. Lanyi. 1999. Structure of bacteriorhodopsin at 1.55 Å resolution. *J. Mol. Biol.* 291:899–911.

Marsh, D. 1997. Dichroic ratios in polarized Fourier transform infrared for nonaxial symmetry of β-sheet structures. *Biophys. J.* 72:2710–2718.

Marsh, D. 1998. Nonaxiality in infrared dichroic ratios of polytopic transmembrane proteins. *Biophys. J.* 75:354–358.

Marsh, D. 1999. Spin label ESR spectroscopy and FTIR spectroscopy for structural/dynamic measurements on ion channels. *Methods Enzymol.* 294C:59–92.

Miyazawa, T. 1960. Perturbation treatment of the characteristic vibrations of polypeptide chains in various configurations. *J. Chem. Phys.* 32: 1647–1652.

Miyazawa, T., and E. R. Blout. 1961. The infrared spectra of polypeptides in various conformations: amide I and II bands. *J. Am. Chem. Soc.* 83:712–719.

Nabedryk, E., and J. Breton. 1981. Orientation of intrinsic proteins in photosynthetic membranes—polarized infrared-spectroscopy of chloroplasts and chromatophores. *Biochim. Biophys. Acta.* 635:515–524.

Parry, D. A. D., and E. Suzuki. 1969. Intrachain potential energy of the α-helix and of a coiled coil strand. *Biopolymers.* 7:189–197.

Reisdorf, W. C. Jr., and S. Krimm. 1995. Infrared dichroism of amide I and amide II modes of α_I- and α_{II}-helix segments in membrane proteins. *Biophys. J.* 69:271–273.

Rothschild, K. J., and N. A. Clark. 1979. Polarized infrared spectroscopy of the purple membrane. *Biophys. J.* 25:473–488.

Sandeman, I. 1955. Amide bands in infra-red spectra: the direction of the transition moments of bands in *N,N′*-diacetylhexamethylenediamine. *Proc. Roy. Soc. A.* 232:105–113.

Schmitt, F.-J., and M. Müller. 1997. Conformation and orientation analysis of modified polyglutamates in thin films by ATR infrared spectroscopy. *Thin Solid Films.* 310:138–147.

Suzuki, E. 1967. A quantitative study of the amide vibrations in the infra-red spectrum of silk fibroin. *Spectrochim. Acta.* 23A:2303–2308.

Tamm, L. K., and S. A. Tatulian. 1997. Infrared spectroscopy of proteins and peptides in lipid bilayers. *Q. Rev. Biophys.* 30:365–429.

Tsuboi, M. 1962. Infrared dichroism and molecular conformation of α-form poly-γ-benzyl-L-glutamate. *J. Polymer Sci.* 59:139–153.

Zbinden, R. 1964. Infrared Spectroscopy of High Polymers. Academic Press, New York.